A BLIND QUALITY MEASURE FOR INDUSTRIAL 2D MATRIX SYMBOLS USING SHALLOW CONVOLUTIONAL NEURAL NETWORK

Zhaohui Che[†], *Guangtao Zhai*[†], *Jing Liu*[‡], *Ke Gu*[*], *Patrick Le Callet*[§], *Jiantao Zhou*[¶] *and Xianming Liu*[£]

[†]Institute of Image Commu. and Network Engin., Shanghai Jiao Tong University, China;
[‡]Tianjin University, China; [*]Beijing University of Technology, China;
[§]Polytech Nantes, France; [¶]University of Macau, China; [£]Harbin Institute of Technology, China;
Email: {chezhaohui, zhaiguangtao}@sjtu.edu.cn

ABSTRACT

Industrial two-dimensional (2D) matrix symbols are ubiquitous throughout the automatic assembly lines. Most industrial 2D symbols are corrupted by various inevitable artifacts. State-of-the-art decoding algorithms are not able to directly handle low-quality symbols irrespective of problematic artifacts. Degraded symbols require appropriate preprocessing methods, such as morphology filtering, median filtering, or sharpening filtering, according to specific distortion type. In this paper, we first establish a database including 3000 industrial 2D symbols which are degraded by 6 types of distortions. Second, we utilize a shallow convolutional neural network (CNN) to identify the distortion type and estimate the quality grade for 2D symbols. Finally, we recommend an appropriate preprocessing method for low-quality symbol according to its distortion type and quality grade. Experimental results indicate that the proposed method outperforms state-of-the-art methods in terms of PLCC, SRCC and RMSE. It also promotes decoding efficiency at the cost of low extra time spent.

Index Terms**—** 2D Matrix Symbol, Image Quality Assessment, Convolutional Neural Network.

1. INTRODUCTION

2D matrix symbols have been widely applied to automated identification applications such as semiconductor wafer marking, industrial components retrospect, and document labels [1, 2]. Compared to 1D barcode, 2D matrix symbols have more attractive advantages, such as large data capacity, compact size, and built-in error checking/correction mechanism [3]. With the development of smartphone, most common 2D matrix symbols in current daily life can be decoded rapidly and accurately. However, how to decode the industrial 2D matrix symbols quickly and reliably is still a challenging task, and it has become a critical topic in machine vision community. Most industrial symbols suffer from problematic artifacts including rough printing surfaces, limited marking techniques, poor lighting conditions, motion blur, scratches and smears, as shown in Fig.1.

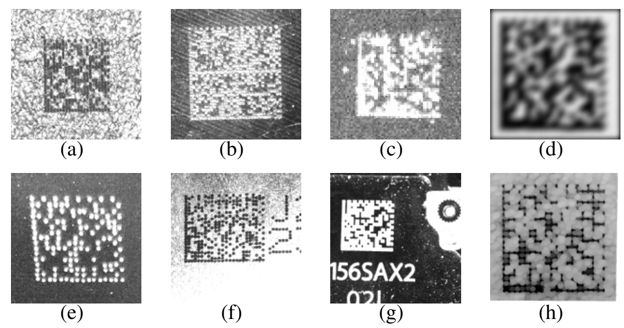

Fig. 1. Some low-quality industrial 2D matrix symbols. Observation indicates that: (a)-(c) are corrupted by severe noise; (d) is degraded by severe motion blur; (e)-(f) are corrupted by geometric deformations, i.e. grid and axial nonuniformities; (g)-(h) are degraded by overprint and underprint artifacts respectively.

Motivation: To the best of our knowledge, known decoding algorithms such as ZXing [4], Zbar [5], libdmtx [6] and 2DTG [7] cannot directly decipher degraded symbols irrespective of problematic distortions. This requires some preprocessing methods based upon the specific distortion types of symbols. Some traditional machine vision-based decoding apparatuses, such as KEYENCE SR-1000 and COGNEX DataMan, have proposed a few preprocessing techniques suitable for industrial symbols [3, 8]. Specifically, for each low-quality symbol, KEYENCE SR-1000 captures thousands of sample images from it by adjusting exposure time, optical gain, and polarization filter, whereafter each sample image is processed by 7 common image filters including smoothing, dilation, erosion, opening, closing, median and sharpening filters. Then each filtered image is passed to decoding step to judge if the symbol can be deciphered successfully. This exhaustive search strategy is reliable, but would be necessarily time-consuming. How to quickly and automatically recommend an appropriate preprocessing method according to specific distortion type of degraded symbols would be meaningful, and promote throughput of assembly lines. Besides, for some symbols with very poor quality, decoding apparatuses still cannot decipher them successfully, although all preprocessing methods have been exhaustively tried. Such case would be expensive in terms of decoding time.

Related Work: Previous research can be divided into two categories. On the one hand, international standardization organization (ISO) disclosed two standards, i.e. ISO-15415 and ISO-16022 [9, 10], to classify the quality of 2D data matrix symbols into 5 grades based on some hand-crafted features. These standards can be regarded as full-reference metrics, because they require a reference decoding algorithm to decipher 2D symbols in advance. However, these standards result in a longer quality estimation time. We refer the readers to [9, 10] for more details. On the other hand, Chen *et al.* proposed a no-reference quality measure for the mobile phone captured 2D barcodes in order to reject the symbols with poor quality [11]. They further improved their work and proposed a reduced-reference quality metric [12]. However, these metrics are limited to only blur and illumination artifacts.

Contribution: Main contribution of this paper includes 3 aspects: 1) We establish a database containing 3000 industrial 2D symbols degraded by 6 types of distortions for the first time; 2) We propose an end-to-end blind quality measure using a shallow CNN architecture, whereby we can determine the distortion type and estimate the quality grade for degraded symbols, and the proposed model is robust to different rotation angles; 3) The proposed method can be applied to two practical applications for promoting decoding efficiency.

2. PROPOSED METHOD

2.1. Industrial 2D Data Matrix Database

As far as we know, there is still no open database with respect to industrial 2D matrix symbols. Notably, quick response code (QR code) and Data Matrix code are two of the most popular 2D matrix symbols. QR code is widely applied for civil use, while Data Matrix code is more suitable to be printed in industrial components, because Data Matrix possesses the smaller dimension compared to other formats. Hence, we select Data Matrix code as research object in this paper.

We select 100 pristine Data Matrix images as reference group. The reference group is made up of 25 symbols printed on glossy metal surfaces, 25 symbols printed on frosted metal surfaces, 25 symbols printed on resin surfaces, and 25 computer-generated symbols produced by encoder software libdmtx [6]. For making sure that the reference group undergos no obvious artifacts, most pristine images are captured by machine vision-based decoding apparatus KEYENCE SR-1000 under the optimal illumination conditions.

We choose 6 typical distortions to simulate artifacts during the process of symbol marking and symbol imaging stages, explained blow: 1) We select 5 levels of Speckle Noise to simulate the artifacts caused by rough printing surfaces; 2) We consider 5 levels of Motion Blur to simulate the artifacts caused by conveyor belts; 3) We consider 5 levels of overprint [10] and 5 levels of underprint [10] to simulate the artifacts caused by limited marking techniques; 4) To simulate grid nonuniformity [9] caused by bad photographing angles, we degrade symbols by 5 levels of perspective transformations; 5) We consider 5 levels of axial stretches to simulate the axial nonuniformity [9]. This way, we derive 30 distorted images for each pristine symbol, and a total of 3000 samples are included in the proposed database[1]. We further augment the database in next section to reduce overfitting.

2.2. Data Annotation, Augmentation and Normalization

Annotation: In this paper, we pay attention to two properties of 2D symbols, i.e. distortion type and quality grade. It's easy to discriminate different distortion types, but how to annotate the quality grades for 2D symbols is debatable. An intuitive sense is that the quality of 2D symbols includes only two levels, i.e. either decodable, or undecodable. However, in reality, some symbols degraded by severe artifacts would be decoded under some "lucky" conditions, such as providential illumination, photographing angle, and powerful error correction system. But this case would result in unstable and unsafe effect because wrongly deciphered results are devastating compared to undecodable. Therefore, we classify the quality of symbols into 5 discrete grades using the full-reference metric defined by ISO-15415 and ISO-16022. Specifically, grade-4 means the best quality level, grade-3, 2 and 1 belong to decodable symbols which are degraded by different distortion levels, and all undecodable symbols are annotated by grade-0. The adopted decoding software is the powerful 2DTG [7].

Augmentation: Data augmentation is necessary to reduce overfitting. Previous works [13,14] used to divide the training images into several patches to extent database content. This method results in 2 defects: 1) The annotation of different patches within the same image would be different, and this would introduce training label noise; 2) Convolution computation of several patches is expensive in terms of inference time. Thus, we enlarge the database by rotating the 2D symbols with 11 different angles. This method is driven by 2 considerations: 1) Different rotation angles have no obvious influences on quality labels of 2D symbols. In other word, rotation is a label-preserving transformation for 2D symbols; 2) This method can promote the robustness of the proposed model to different rotation angles. This way, we derive 33K images in total.

Normalization: The normalization step guarantees that all images of the proposed database have the same resolution (256×256) and the same polarization (i.e. finder pattern of symbols are dark, while background of symbols are bright).

2.3. The CNN Architecture

Inspired by previous works [14, 15], we decompose the blind quality prediction problem into two subtasks. Subtask I classifies an degraded symbol into a specific distortion type from a set of pre-defined categories, as mentioned in section 2.1. Subtask II classifies the same symbol into a specific quality

[1]The proposed database can be downloaded from: https://mega.nz/#F!Zi4nlTSR!MU-JWzBEoZHxqkFSxJA_Jg

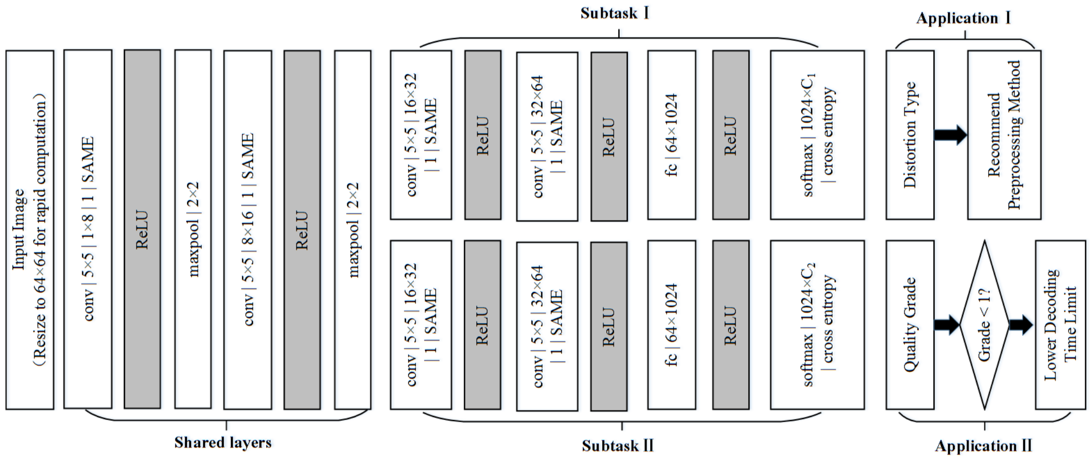

Fig. 2. Flowchart of the proposed CNN architecture. We follow the style and convention in [15] to represent the parameterization of the convolutional layer as "height×width | input channel×output channel | stride | padding", and "fc" means "fully connected layer". Besides, C_1 and C_2 denote the total number of categories of the predefined distortion types and quality grades, respectively.

grade from 5 levels defined by ISO-15415 and ISO-16022 [2].

Shared layers: As shown in Fig.2, subtask I and subtask II share the first two convolutional layers which contain 8 and 16 kernels respectively, followed by a Rectified Linear Unit (ReLU) activation function and a 2×2 max pooling. This architecture is motivated by two considerations: 1) shared layers can save computational expense, and 2) learning multiple correlated tasks at the same time may promote the performance of the main task [16].

Subtask I: On top of the shared layers, subtask I appends two convolutional layers including 32 and 64 kernels respectively, and one fully connected layer containing 1024 neurons. We use $\mathbf{h}^{(\mathrm{k})}$ to represent the deep features from the last fully connected layer, where k means the k-th input image of mini-batch training data set. Then we append a softmax layer to map $\mathbf{h}^{(\mathrm{k})}$ to a C_1-dimensional probability vector $\mathbf{p}^{(\mathbf{k})} = [\mathrm{p}_1^{(\mathrm{k})}, \mathrm{p}_2^{(\mathrm{k})}, ..., \mathrm{p}_{\mathrm{C}_1}^{(\mathrm{k})}]$, in which the maximal probability indicates the predicted distortion type. Suppose that $\mathbf{W}$ and $\mathbf{b}$ represent the weights and biases of the softmax layer, we obtain the unnormalized probability vector as $\mathbf{z}^{(\mathrm{k})} = \mathbf{W}^{\mathsf{T}}\mathbf{h}^{(\mathrm{k})} + \mathbf{b}$, where $\mathbf{z}^{(\mathrm{k})} = [\mathrm{z}_1^{(\mathrm{k})}, \mathrm{z}_2^{(\mathrm{k})}, ..., \mathrm{z}_{\mathrm{C}_1}^{(\mathrm{k})}]$. Then we use equation 1 to derive the normalized probability vector.

$$\mathrm{p}_{\mathrm{i}}^{(\mathrm{k})} = \frac{\mathbf{exp}(\mathrm{z}_{\mathrm{i}}^{(\mathrm{k})})}{\sum_{\mathrm{j}=1}^{\mathrm{C}_1} \mathbf{exp}(\mathrm{z}_{\mathrm{j}}^{(\mathrm{k})})}, \mathrm{i} \in \{1, 2, ..., \mathrm{C}_1\}, \tag{1}$$

For subtask I, we empirically select cross entropy as loss:

$$\boldsymbol{l}_1 = -\sum_{\mathrm{k}=1}^{\mathrm{K}} \sum_{\mathrm{i}=1}^{\mathrm{C}_1} \mathrm{p}_{\mathrm{i}}^{(\mathrm{k})} \mathbf{log} \bar{\mathrm{p}}_{\mathrm{i}}^{(\mathrm{k})}. \tag{2}$$

where K means the mini-batch size of the training data, which is set as 100 here. Besides, $\bar{\mathrm{p}}_{\mathrm{i}}^{(\mathrm{k})}$ represents the training label of the i-th distortion type of the k-th input training image.

Subtask II: Notably, we tried to use a similar CNN architecture as [15] to share all convolutional layers with two subtasks, but the performance is unsatisfying. The reasons include 2 aspects: 1) each distortion type of the proposed database is homogeneous across the entire image, and discrepancies between different distortion types are distinct; 2) quality grade of industrial 2D symbol does not completely depend on distortion type. In fact, it may be affected by complex factors, such as data modulation ratio decline and finder pattern damage caused by incidental issues [9]. Moreover, the discrepancies between a pair of 2D symbols with adjacent quality grades are not very conspicuous. Therefore, for subtask II, we separate the 3rd and 4th convolutional layers with subtask I, and individually train a sub-network for better prediction accuracy. The output of sub-network II is a softmax layer, which is responsible for mapping the 1024-dimensional deep features to a C_2-dimensional probability vector $\mathbf{q}^{(\mathbf{k})} = [\mathrm{q}_1^{(\mathrm{k})}, \mathrm{q}_2^{(\mathrm{k})}, ..., \mathrm{q}_{\mathrm{C}_2}^{(\mathrm{k})}]$, in which the maximal probability indicates the predicted quality grade. The empirical loss function used here is cross entropy: $\boldsymbol{l}_2 = -\sum_{\mathrm{k}=1}^{\mathrm{K}} \sum_{\mathrm{i}=1}^{\mathrm{C}_2} \mathrm{q}_{\mathrm{i}}^{(\mathrm{k})} \mathbf{log} \bar{\mathrm{q}}_{\mathrm{i}}^{(\mathrm{k})}$, where $\bar{\mathrm{q}}_{\mathrm{i}}^{(\mathrm{k})}$ represents the training label of the i-th quality grade of the k-th input training image.

Training: Different from traditional multi-task learning methods which use an overall loss function to optimize parameters [14–16], the training stage in this paper is divided into two stages. Considering that subtask I is much easier to learn, we first feed the augmented training samples to train the sub-network I by minimizing loss function $\boldsymbol{l}_1$. Second, we use parameters of the 1st and 2nd convolutional layers obtained in the first stage to initialize the weights and biases of the shared layers. Then we further optimize the rest layers of sub-network II by minimizing loss function $\boldsymbol{l}_2$. Adaptive moment estimation (Adam) with a fixed learning rate $\mathrm{lr} = 1 \times 10^{-3}$ serves as an optimization function to minimize the loss func-

[2] Notably, contrast change distortion has not been considered in this paper due to its heavy complexities. For reducing effect of contrast distortion to final quality grade of 2D symbol, we omit "symbol contrast" feature defined by [9, 10] when annotating quality label.

Table 1. Distortion classification accuracy for each distortion type. All models are trained and tested on the proposed 2D symbols database. The best performances are highlighted by red.

	S-Noise	M-Blur	O-Print	U-Print	GrNu	AxNu	Overall
AlexNet [17]	0.880	0.873	0.876	0.794	0.814	0.719	0.826
IQA-CNN++ [14]	0.665	0.734	0.703	0.622	0.724	0.580	0.671
MEON [15]	0.933	0.971	0.866	0.789	0.869	0.790	0.869
Proposed	0.958	0.882	0.919	0.813	0.904	0.801	0.880

Table 2. Performance of quality grade estimation task.

	PLCC	SRCC	RMSE	Model Size
AlexNet [17]	–	–	–	6000×10^4
IQA-CNN++ [14]	0.6229	0.6092	1.1158	7.9×10^4
MEON [15]	0.7518	0.7556	0.8151	10.6×10^4
SSIM [18]	0.5584	0.5141	1.1535	–
Proposed	0.8206	0.8068	0.7312	16.6×10^4

tions, because Adam occupies the less CPU/GPU memory resource, and achieves a better prediction accuracy compared to SGD (stochastic gradient descent) in our tasks. Training and testing codes of the proposed method are available here[3].

3. EXPERIMENTAL RESULTS

Distortion Classification: Table 1 shows the distortion classification accuracy of different methods on the proposed database, where S-Noise, M-Blur, O-Print, U-print, GrNu and AxNu represent different distortion types, i.e. Speckle-Noise, Motion-Blur, Over-Print, Under-Print, Grid-Nonuniformity and Axial-Nonuniformity, respectively. We perform a 5-fold cross-validation for fair comparison. In each validation round, the database is randomly divided into 5 folds, where 4 folds serve as training set and the remaining 1 fold serves as testing set. Experimental results indicate that the proposed model outperforms state-of-the-art methods. However, the performance on AxNu is not satisfying, and we find that most False Negatives of AxNu are wrongly classified as GrNu. Besides, MEON achieves the best performance on M-Blur.

Quality Grade Prediction: Table 2 shows the quality grade prediction performance of different methods, where "Model Size" represents the amount of parameters to be learned in the network. Considering that SSIM is a traditional full-reference quality metric, here we first adopt a logistic regression function $\bar{\mathrm{S}} = \beta_1(\frac{1}{2} - \frac{1}{1+\mathbf{exp}(\beta_2(\mathrm{S}-\beta_3))}) + \beta_4\mathrm{S} + \beta_5$ to map the original quality grade S to $\bar{\mathrm{S}}$, as suggested by video quality experts group (VQEG) [19–23]. Besides, $\beta_\lambda(\lambda \in \{1, 2, ..., 5\})$ are free parameters to be determined during the curve fitting process. Then we use the mapped quality score $\bar{\mathrm{S}}$ to compute 3 popular evaluation criteria including Pearson liner correlation coefficient (PLCC), Spearman's rank order correlation coefficient (SRCC), and Root mean squared error (RMSE) for fair comparison. The proposed method achieves a top ranked performance at the cost of a few more trainable parameters.

[3] https://github.com/CZHQuality/BQAfor2DSymbols

Table 3. Accuracy of dividing 2D symbols into two categories, i.e. decodable and undecodable. The 1st and 2nd rows represent the decoding time of libdmtx when dealing with 2D symbols with the best (grade-4) and the worst (grade-0) quality grades.

	Accuracy	FAR	FRR	Time Cost
libdmtx [6]: quality = 4	–	–	–	$\approx$ 28 ms
libdmtx [6]: quality = 0	–	–	–	$\geq$ 500 ms
Chen's method [12]	0.818	0.088	0.094	$\approx$ 5.5 ms
Proposed	0.944	0.024	0.032	$\approx$3.33 ms

4. APPLICATION

Preprocessing Method Recommendation: The proposed method provides a rapid and automatical preprocessing methods selection strategy. As mentioned in motivation part, 2D symbols with different distortions require appropriate preprocessing methods. Empirically speaking, smoothing filter handles S-Noise well, sharpening filter handles M-Blur well, morphological operations perform well on O-Print and U-Print, perspective transform is valid to GrNu, and grid-correction handles AxNu well. As shown in Fig.2, the output of sub-network I is a C_1-dimensional probability vector $\mathbf{p}^{(\mathrm{k})}$, in which the maximal probability indicates the predicted distortion type. We rank the preprocessing methods according to the numerical values within $\mathbf{p}^{(\mathrm{k})}$, in order to save preprocessing time compared to traditional exhaustive approach [3].

Time Limit Adjustment: Inspired by Chen's work [12], we use the proposed network to divide 2D symbols into two categories (simply change C_2 from 5 to 2, and retrain the network), i.e. decodable (quality grade > 0) and undecodable (quality grade $= 0$). Table 3 shows the classification results and time cost (for single image) of different methods. The time cost is measured on a desktop computer with Intel Core I7 CPU, NVIDIA GTX 690 GPU, and Python 2.7 environment. For symbols with very bad quality, decoding software like libdmtx will not stop exhaustive search until time limit (500 ms) has run out, and this is expensive in terms of time. Hence, for saving time, we use the proposed model to estimate the quality grade in advance, and set a lower decoding time limit for symbols predicted as undecodable.

5. CONCLUSION

We propose a blind quality measure for industrial 2D symbols using a shallow CNN architecture, which divides the quality measure problem into two subtasks, i.e. distortion type classification and quality grade estimation. The proposed method achieves the top ranked performances on two subtasks, and is robust to different rotation angles. Besides, the proposed model can be applied to two practical applications for improving decoding efficiency at the cost of low extra time spent. We share the proposed database and code with the community to facilitate next research.

6. ACKNOWLEDGEMENT

This work was supported by the National Science Foundation of China (61521062, 61527804) and Science and Technology Commission of Shanghai Municipality (15DZ0500200), and the Macau Science and Technology Development Fund under Grant FDCT/022/2017/A1.

7. REFERENCES

[1] C. Chu, D. Yang, and M. Chen. "Image stabilization for 2d barcode in handheld devices". In *ACM international conference on Multimedia (ACM MM)*, 2007, pp. 697-706. 1

[2] D. Mejias, I. Diaz, and F. Maria. "A low-complexity pre-processing system for restoring low-quality qr code images". *IEEE Transactions on Consumer Electronics (T-CE)*, vol. 57, no. 3, August 2011. 1

[3] S. Nadabar and R. Desai. "Method and apparatus using intensity gradients for visual identification of 2d matrix symbols". In *U.S. Patent, US 6941026B1*, 2005. 1, 4

[4] Zxing: Open source barcode scanning library. https://github.com/zxing/zxing. 1

[5] Zbar: Open source software suite for reading bar codes. https://github.com/ZBar/ZBar. 1

[6] libdmtx: Open source datamatrix decoding software. http://libdmtx.sourceforge.net/. 1, 2, 4

[7] 2dtg: Business software for decoding barcode. https://www.2dtg.com/. 1, 2

[8] C. Natsukari and H. Nakata. "Two-dimensional code reader setting method, two-dimensional code reader, two dimensional code reader setting program and computer readable recording medium". In *U.S. Patent, US 6983886*, 2006. 1

[9] "Information technology – automatic identification and data capture techniques – bar code symbol print quality test specification – two-dimensional symbols". In *ISO/IEC-15415*, 2011. 2, 3

[10] "Information technology – automatic identification and data capture techniques – data matrix bar code symbology specification". In *ISO/IEC-16022*, 2006. 2, 3

[11] C. Chen, A. Kot, and H. Yang. "A quality measure of mobile phone captured 2d barcode images". In *IEEE International Conference on Image Processing (ICIP)*, 2010, pp. 329-332. 2

[12] C. Chen, A. Kot, and H. Yang. "A two-stage quality measure for mobile phone captured 2d barcode images". *Pattern Recognization (PR)*, vol. 46, no. 9, August 2013. 2, 4

[13] L. Kang, P. Ye, Y. Li, and D. Doermann. "Convolutional neural networks for no-reference image quality assessment". In *IEEE Conference on Computer Vision and Pattern Recognition (CVPR)*, 2014, pp. 1733-1740. 2

[14] L. Kang, P. Ye, Y. Li, and D. Doermann. "Simultaneous estimation of image quality and distortion via multi-task convolutional neural networks". In *IEEE International Conference on Image Processing (ICIP)*, 2015, pp. 2791-2795. 2, 3, 4

[15] K. Ma, W. L, K. Zhang, Z. Duanmu, Z. Wang, and W. Zuo. "End-to-end blind image quality assessment using deep neural networks". *IEEE Transactions on Image Processing (T-IP)*, vol. 27, no. 3, March 2018. 2, 3, 4

[16] R. Caruana. "Multitask learning". *In Learning to learn*, 1998, pp. 95-133. 3

[17] A. Krizhevsky, I. Sutskever, and G.E. Hinton. "Imagenet classification with deep convolutional neural networks". In *Advances in neural information processing systems (NIPs)*, 2012, pp. 1097-1105. 4

[18] Z. Wang, A.C. Bovik, H.R. Sheikh, and E.P. Simoncelli. "Image quality assessment: from error visibility to structural similarity". *IEEE Transactions on Image Processing (T-IP)*, vol. 13, no. 4, April 2004. 4

[19] A.M. Rohaly, J. Libert, P. Corriveau, and A. Webster. "Final report from the video quality experts group on the validation of objective models of video quality assessment". In *ITU-T Standards Contribution COM*, 2000. 4

[20] Z. Che, G. Zhai, K. Gu, and P.L. Callet. "A reduced-reference quality metric for screen content image". In *IEEE International Conference on Image Processing (ICIP)*, 2017, pp. 1852-1856. 4

[21] X. Min, K. Ma, K. Gu, and G. Zhai. "Unified?blind quality assessment of compressed natural, graphic, and screen content images". *IEEE Transactions on Image Processing (T-IP)*, vol. 26, no. 11, April 2017. 4

[22] X. Min, K. Gu, and G. Zhai. "Blind quality assessment based on pseudo reference image". *IEEE Transactions on Multimedia (T-MM)*, 2017. 4

[23] G. Zhai, X. Wu, X. Yang, and W. Zhang. "A psychovisual quality metric in free-energy principle". *IEEE Transactions on Image Processing (T-IP)*, vol. 21, no. 1, Jan, 2012. 4